Egyptian Journal of Chemistry

http://ejchem.journals.ekb.eg/

Electric Modulus and Scaling Behaviour of Chitosan/PVA Biopolymer Blend

M. T. Ahmed [*1,2], H. Elhendawy[3], Z. M. Elqahtani[4], Wafaa Bakr Elsharkawy[1], M. A. Azzam[5], Tarek Fahmy[1,2]

[1]*Dept. of Physics, College of Science and Humanities in Al-Kharj, Prince Sattam bin Abdulaziz University, AlKharj 11942, Kingdom of Saudi Arabia.*

[2]*Polymer Research Group, Physics Dept., Faculty of Science, Mansoura University, 35516*

[3]*Department of Basic Science, Delta Higher Institute for Engineering and Technology, 11152 Mansoura, Egypt*

[4]*Dept. of Physics, College of Science, Princess Nourah bint Abdulrahman University, Ryiadh, Saudi Arabia*

[5]*Chemistry Department, College of Science and Humanities,*

Abstract

Dielectric measurements of chitosan/PVA polymer blends were performed at various temperatures in a wide frequency range. Higher values of ε' and ε'' at higher temperatures and lower frequencies are correlated to interfacial polarization (IP) and DC conduction, respectively. Isochronal behavior of // against temperature revealed that chitosan and PVA is characterized by a dipolar relaxation peak at T= 393 K and 348 K, respectively. The activation energy (Ea) values of conduction have been estimated for all samples. Cole-Cole behavior revealed that, with increasing the temperature the semicircles area of the samples increased and the semicircle intercept are shifted towards higher value of / indicating that, the capacitance is increased. Complex electric modulus (M*) of all samples is investigated and it is found that, real part (M/) of the complex electric modulus showed nonlinear behavior with frequency, whereas, (M//), i.e., the imaginary part, is characterized by a relaxation peaks for all samples. The scaling behavior has been carried out at T= 333 K, as a representative temperature and it is found that, all the curves are overlapped leading to a master curve indicating that, dynamic process is temperature independent.

Keywords: Chitosan, PVA, Electric modulus, Relaxation, Scaling.

Introduction

Chitosan (Cs) is considered as a linear polysaccharide consists of $\beta(1\rightarrow4)$-2-amino-2-deoxy-D-glucopyranose (D-glucosamine) and $\beta(1\rightarrow4)$-2-acetamido-2-deoxy-D-glucopyranose (*N*-acetyl-D-glucosamine). Chitosan is derived from chitin by treating it with aggressive deacetylation solution. Chitin can be obtained from crustacean shells, meaning that chitosan and chitin are examples of renewable resources [1]. Since chitosan contains functional groups such as hydroxyl, amides and amines, which act as hydrogen bond acceptors or donors, they are likely to be linked with hydrogen bond acceptor or donor compound.

PVA is a semi-crystalline, water-soluble in nature, flexible hydrophilic network, low cost and non-toxicity. It is characterized by good charge storage capacity and a high dielectric permittivity. These characteristics make PVA is an interesting polymer [2]. PVA has also gained massive and growing interest in the biomedical field due to its bio-inertness [3]. Interestingly, the new materials are polymer blends, that is, materials that consist of several components and have new qualitative properties that differ from those of pure individual components. Polymer blending has attracted much interest in development and research in polymer science over the past decades, due to its potential use in many applications, such as, membranes, sensors and shielding [4-6]. Chitosan and PVA have many applications in cosmetic industry, medicine and pharmacy because of their non-toxicity, biodegradability and biocompatibility [7]. The hydrogen bonding interactions between hydroxyl

*Corresponding author e-mail: moustf_1@yahoo.com.; (M. T. Ahmed).
Receive Date: 24 June 2021, Revise Date: 19 July 2021, Accept Date: 02 August 2021
DOI: 10.21608/EJCHEM.2021.81068.4015

groups and amino of the chitosan and OH groups of PVA are responsible for the compatibility and miscibility of both chitosan and PVA [8].

Dielectric relaxation spectroscopy is a powerful technique to investigate dielectric relaxation phenomena, structure and molecular rotational dynamics in polymeric materials [9-15]. Knowing the dielectric parameters of polymers, such as dielectric constant and dielectric loss is absolutely essential for their application in the manufacture of any type of electronic devices. Research on polymers for the application of high temperature dielectric is mostly focused on improving thermal stability and dielectric properties, such as high glass transition temperature (T_g) and high dielectric constant, respectively. Many dielectric measurements of polysaccharides have been discussed controversially regarding number of relaxation process, behavior of the dielectric spectra and their interpretations [16]. The main reasons for discussion are water content effect and highly complex super-molecular structure of polysaccharide, such as, intra and intermolecular hydrogen bond. In our previous work, morphology, FTIR and TGA of chitosan/PVA biopolymer polyblend are investigated intensively and it is found that this polyblend is partially compatible to each other. In addition, AC conductivity measurements showed that, behavior of AC conductivity mechanism is consistent with the model of overlapping-large polaron tunneling (OLPT), whereas, behavior of dielectric loss tangent displayed two distinct relaxation processes with different activation energy values [17]. This manuscript is devoted to shed light on behavior of complex electric modulus to calculate the activation energy and relaxation time of different relaxation processes. Another aim of this manuscript is to investigate the dynamic process of chitosan/PVA polyblend using scaling behavior.

2 Experimental Work

Materials and Films Preparation

Chitosan was obtained from Sigma-Aldrich with deacetylation degree, (DD) ~ 75%. Poly (Vinyl Alcohol), $(C_2H_4O)_n$ with molecular weight, M_w ~ 72,000, density 1.26 g/cm^3 and hydrolysis degree of ~ 99 mol% was obtained from Merck. Chitosan, PVA and its polyblend samples were obtained by dissolving them in aqueous solution containing 6% acetic acid. The solution was then stirred for one day at room temperature to ensure homogeneity as well as solubility. The resulting solution at a temperature of 348 K is poured in the oven for one day in well-cleaned petri dishes. Fig. 1 describes suggested chemical interaction between PVA and chitosan.

Measurements

Samples of chitosan, PVA and its polyblend are kept short-circuited for at least 30 minutes at each temperature to remove the stray charges prior to the measurements. Lock-in amplifier model SR 830, (Stanford Research System) is used to record the measurements of dielectric properties and electrical conductivity. The measurements are very sensitive to the surrounding atmosphere humidity, hence, system of the measurements is evacuated at ~ 10^{-4} Torr because of wet nature of the materials. Dielectric measurements are recorded in the frequency range from 10^{-1} Hz to 10^5 Hz at various temperatures in the range of ~ 298 K to 423 K.

Results and Discussion

Dielectric constant

The dielectric relaxation study gives valuable and sufficient information about orientational and translational motion of mobile charge carriers in the dielectric. The dielectric constant (ε') changes with the frequency dispersion of the applied field and is also dependent on the physical properties of the dielectrics. Variation of the dielectric constant (ε') arose in different frequency domains due to different dielectric polarizations, such as ionic, electronic, interfacial and orientational.

The dielectric constant ε' expresses the charge stored in the material while the dielectric loss ε'' expresses the energy loss when the polarity of the electric field is rapidly reversed. Dielectric properties of frequency dependent of chitosan/PVA polyblend can be described using the complex permittivity, $\varepsilon^*(\omega)$ as follow:

$$\varepsilon^*(\omega) = \varepsilon'(\omega) - j\varepsilon''(\omega) \qquad (1)$$

Where, ε' and ε'' are the dielectric constant and dielectric loss, respectively. The behavior of both ε' and ε'' of chitosan, PVA and its polyblend samples have been investigated in a wide frequency range at various temperatures, as displayed in Figs. 2-3(a&b). In general, it was noticed that all samples were characterized by high dielectric constant and dielectric loss at low frequency and then decreased with increasing frequency, while at high frequency, they appeared to be constant, i.e., frequency independent. The obtained high value of both ε' and ε'' at lower frequencies may be attributed to the charges accumulation at the electrode-sample interface that leads to the electrode phenomena of polarization, or space charge polarization/interfacial polarization (IP) because of the heterogeneity of chitosan/PVA polyblend samples [18-20].

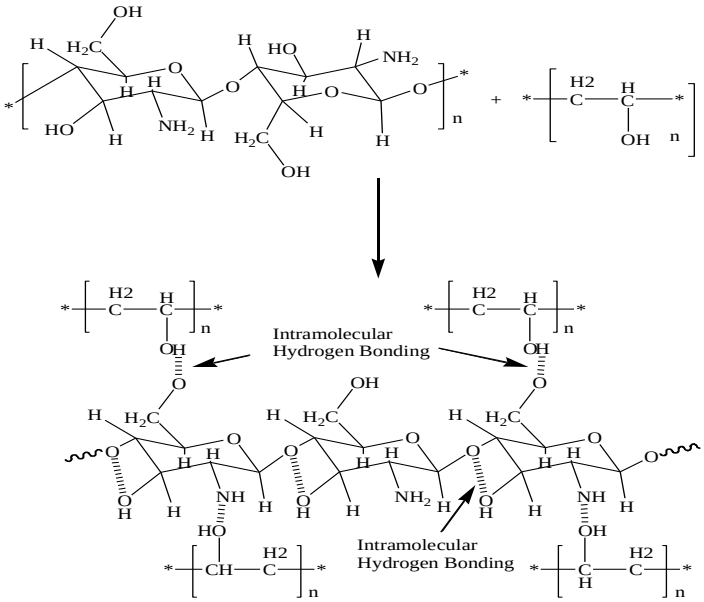

Fig. 1: The suggested chemical interaction between chitosan (Cs) and PVA.

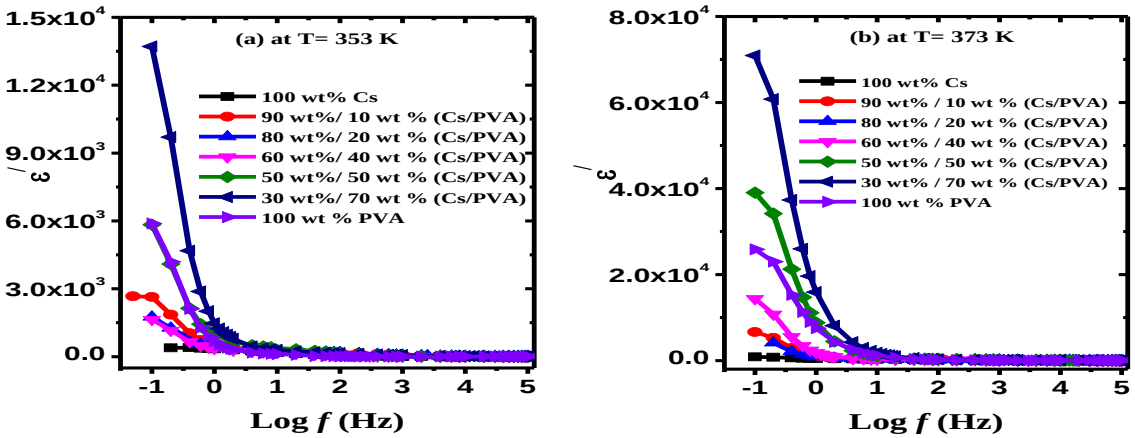

Fig. 2: $\varepsilon^{/}$ against frequency for Cs/PVA samples at a) T= 353 K and b) T= 373 K.

The polymer chain flexibility has an effect on the dielectric constant of the materials at lower frequency and higher temperatures. At lower frequencies, the electric field is slow, and therefore there is a sufficient time for the induced and permanent dipoles to align very well with the applied electric field. Hence, the interfacial polarization (IP), i.e., polarization of Maxwell-Wagner-Sillars (MWS) is enhanced and increased. On the other hand, the low values of $\varepsilon^{/}$ at high frequencies are due to the fact that there is not enough time for the dipoles to align along the electric field. The behavior of $\varepsilon^{/}$ at higher frequencies is dominated by model of micro-capacitor structure, i.e., it becomes independent on frequency and its value remains constant, as shown in Fig. 2(a&b) [21].

It is also evident, as in Fig. 2(a&b) that with increasing temperature the value of the dielectric constant increases. The charge distribution as well as the statistical thermal motion of the polar groups plays a clear role in determining the dielectric behavior of the polymers. The dielectric constant in case of polar polymers starts to decrease at a specific critical frequency and at lower temperatures the dipole molecules cannot orient themselves. The increase of the dielectric constant with temperature may be related to the known phenomenon of increasing the polarization with increasing temperature, as is observed in many materials [22-24]. Increasing the temperature will improve the polymer segmental mobility, hence, facilitates the dipoles orientation and increases the dielectric constant as a result.

Fig. 3(a&b) depicts the dielectric loss ($\varepsilon^{//}$) behavior of all samples at different temperatures. It is observed that, $\varepsilon^{//}$ behavior obeyed the same trend of $\varepsilon^{/}$. It is observed that values of $\varepsilon^{//}$ are increased with temperature while decreasing with increasing frequency, as shown in Fig. 3 (a&b). The high values of dielectric losses observed at lower frequencies are mainly due to DC conduction associated with interfacial polarization, (IP) [25].

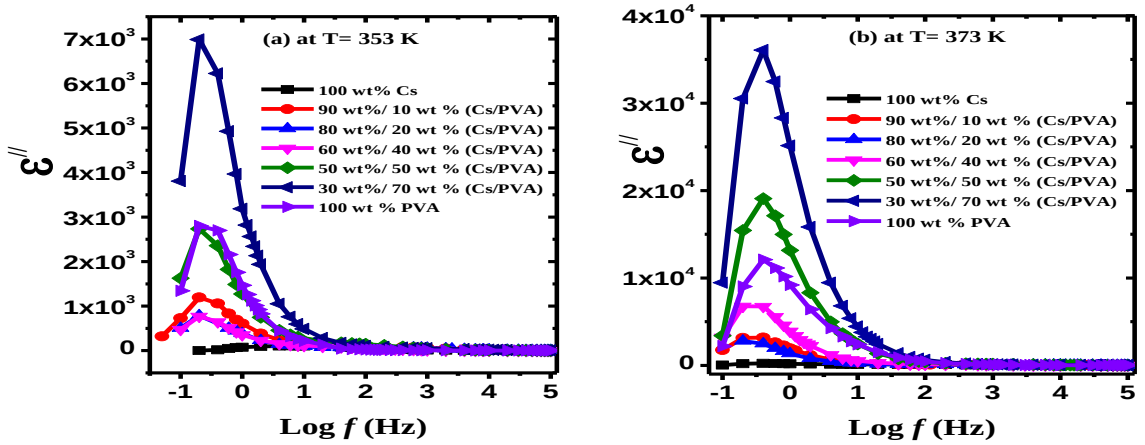

Fig. 3: $\varepsilon^{//}$ against frequency for all samples at a) T= 353 K and b) T= 373 K.

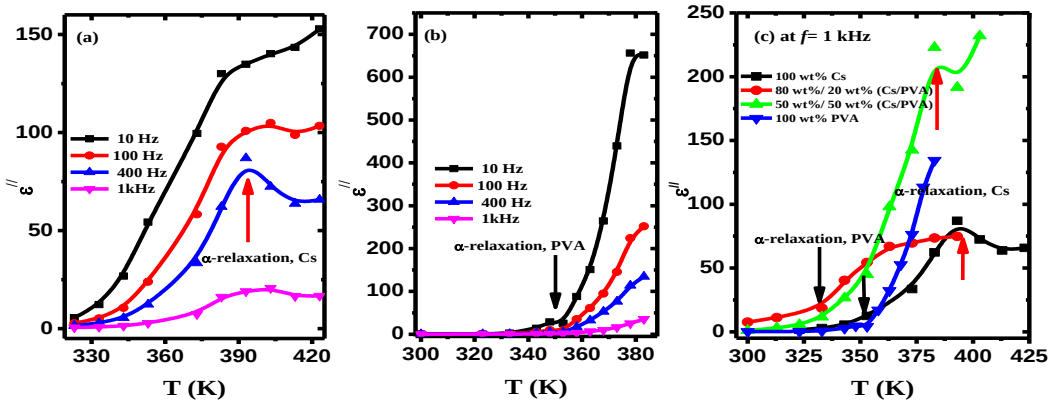

Fig. 4: Isochronal plot of $\varepsilon^{//}$ against temperature at fixed frequencies of a) Cs, b) PVA and c) all the samples at f = 1 kHz.

Fig. 4(a-c) displays variation of $\varepsilon^{//}$ at various frequencies of chitosan (Cs) and PVA against temperature T, and at a fixed frequency ~1 kHz for pure and some polyblend samples, as shown in Fig. 4c. Fig. 4(a&b) revealed that, $\varepsilon^{//}$ behavior is characterized by a broad relaxation peak centered at T= 393 K and a shoulder at T = 348 K for chitosan and PVA, respectively. These relaxation phenomena are observed nearly around the glass transition temperature (T_g) of both chitosan and PVA and assigned as α-relaxation, i.e., dipolar relaxation. The dipolar relaxation of chitosan is related to glass transition and can be explained as torsional oscillations between the reordering of cooperative hydrogen bonds and two glucopyranose rings across a glucosidic oxygen [26]. On the other side, dipolar relaxation of PVA can be attributed to chain segment relaxation involved in hydrogen bonding interactions in the amorphous-crystalline interphase [27]. The chains are irregular and intertwined in the amorphous regions, while the chains are evenly arranged in the crystalline regions. Thus, the molecular chains move easily in the amorphous phase compared to the crystalline phase. Due to the weak molecular packing in the amorphous phase, the density is smaller than that of the crystalline phase. So, the chains in the amorphous phase are more flexible and are able to orient themselves easily and more quickly. As already well known, PVA is a mixture of amorphous and semi-crystalline in nature. Hence, dipolar molecules in the main chain, (Hydroxyl groups, OH) or in the side chains (CH_2) will orient more easily from position to another and it will participate in dielectric loss behavior over a wide range of temperature as well as frequency. The behavior of $\varepsilon^{//}$ is characterized by two different relaxation peaks for polyblend samples and are detected as a shoulder in the vicinity of T_g of PVA and a peak in the vicinity of T_g of chitosan, as shown in Fig. 4c.

The obtained behavior of dielectric loss is typical of polar materials in which the dipole orientation is facilitated with increasing temperature and thus the values of dielectric loss are increased. As the temperature increases, the polymer viscosity begins to decrease slightly, causing the dipole to rotate easily with the applying field, resulting in an increase in the dielectric loss. But the motion of the dipoles increases above T_g due to the continuous rise in temperature, causing the dipoles with higher amplitude to vibrate. As a result, the polarization process will be switched and then the dielectric loss will decrease again.

AC Conductivity

The electrical conductivity of polymers has been extensively investigated currently to interpret the nature of charge transfer in these materials. Polymers are good insulating materials with low value of conductivity, and therefore are of interest to the industry of microelectronics. The electrical conductivity of polymers depends mainly on the thermally generated carriers and/or on the appropriate doping addition in polymer composites.

Fig. 5a displays the behavior of σ_{ac} conductivity of chitosan, PVA and the polyblend samples at T= 373 K in a frequency range from 0.1 Hz to 10^5 Hz. One can observe that, the electrical conductivity of all samples generally increases with increasing frequency and the overall behavior of electrical conductivity can be divided into three regions. The lower values of σ_{ac} below 1 Hz can be attributed to an accumulation of charged species at the electrode-sample interface, which leads to a reduction of mobile charge carriers in the material that contribute to conduction [28]. It is worth mentioning that, the behavior of σ_{ac} of all samples is characterized by a plateau region. The range of this plateau region is enlarged with increasing PVA content in the polyblend samples as indicated by the two arrows in Fig. 5a. Then, the electrical conductivity starts to increase with frequency above 1kHz. This behavior of σ_{ac} conductivity can be explained using Jonscher equation as follow:

$$\sigma(\omega)=\sigma_{dc}+A\omega^{n} \quad (2)$$

Where σ_{dc}, A, ω, and n are DC conductivity, temperature dependent constant and is the measure of polarizability, angular frequency and power parameter which represents the interaction between charges and lattice, respectively. Values of n and A are estimated by knowing the slope and intercept of log σ versus log f at fixed temperature in the high frequency region, as shown in Fig. 5b and listed in Table 1.

It is noticed that, the values of n of all samples are ranged from 0.27 to 0.83. Different models such as, correlated barrier hopping (CBH), overlapping-large polaron tunneling (OLPT) and quantum mechanical tunneling (QMT) have been proposed to interpret the correlation between the exponent n and the temperature (T) [29,30].

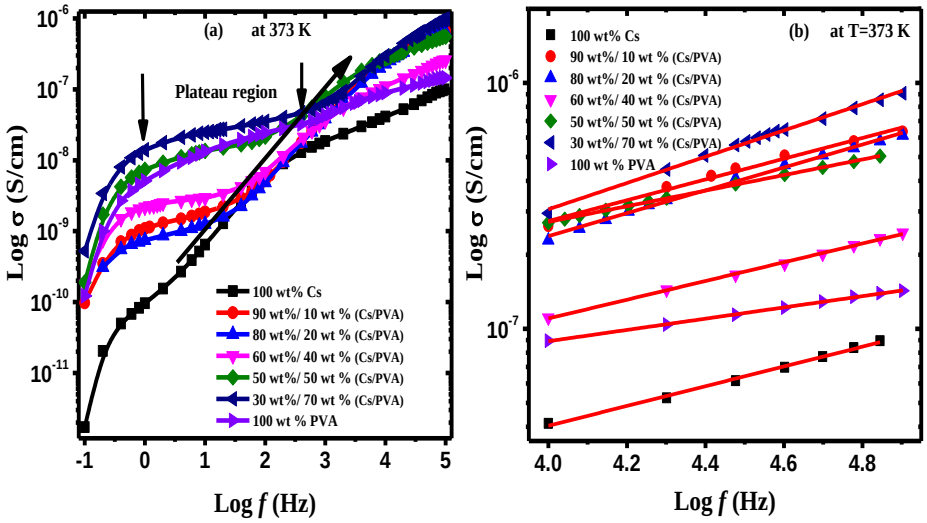

Fig.5: a) The variation of electrical conductivity versus frequency of all samples at T= 33 K. b) Log σ against Log f in the high frequency region according to Jonscher equation.

Fig. 6 displays the variation of both n and A as a function of temperature of pure chitosan and pure PVA. It is found that with increasing in temperature, the values of n decreased in general until it reached a minimum at a certain temperature and begins to increase again with increasing temperature, while the values of A start to increase with the temperature and then decrease again. This behavior confirms that the frequency dependence of electrical conductivity is correlated with the overlapping-large polaron tunneling (OLPT) model [17].

Fig. 7a shows the electrical conductivity dependence of chitosan, PVA and some polyblend samples on the temperature at a fixed frequency, f= 100 Hz. It is found that, the electrical conductivity of all samples increases generally with increasing temperature. This behavior could be attributed to local structural relaxation and polymeric segmental motion. The observed continuous increase in the electrical conductivity of the samples can be attributed to a decrease in the degree of crystallinity, which leads to an increase in the amorphisity after blending of chitosan and PVA. As the amorphous region gradually increases in the polyblend samples, the polymer chain acquires faster internal patterns in which the rotation of the bond produces a segmental motion.

Table 1: Values of the exponent *n* and the constant *A*.

	Chitosan (Cs)		90/10 wt% (Cs/PVA)		80/20 wt% (Cs/PVA)		60/40 wt% (Cs/PVA)		50/50 wt% (Cs/PVA)		30/70 wt% (Cs/PVA)		PVA	
T (K)	*n*	*A*	*n*	*A*	*n*	*A*	*n*	*A*	*n*	*A*	*n*	*A*	*n*	*A*
298	----	----	0.62	$1.44x10^{-11}$	0.64	$3.80x10^{-11}$	0.69	$3.46x10^{-12}$	0.67	$4.46x10^{-12}$	0.72	$1.44x10^{-12}$	0.83	$2.34x10^{-13}$
314	----	----	0.55	$7.07x10^{-11}$	0.58	$8.51x10^{-11}$	0.61	$5.75x10^{-12}$	0.57	$2.34x10^{-11}$	0.64	$6.91x10^{-12}$	----	----
323	0.61	$1.00x10^{-11}$	----	----	0.63	$9.54x10^{-11}$	0.58	$1.25x10^{-11}$	0.53	$5.88x10^{-11}$	0.56	$3.01x10^{-11}$	0.78	$5.75x10^{-13}$
333	0.55	$1.73x10^{-11}$	0.39	$8.12x10^{-10}$	----	----	0.55	$2.69x10^{-11}$	0.47	$2.18x10^{-10}$	0.47	$2.08x10^{-10}$	0.69	$3.09x10^{-12}$
343	0.49	$4.78x10^{-11}$	0.33	$2.29x10^{-09}$	0.45	$9.12x10^{-10}$	0.50	$3.98x10^{-11}$	0.44	$7.24x10^{-10}$	0.43	$9.77x10^{-10}$	0.56	$3.01x10^{-11}$
348	----	----	----	----	----	----	----	----	----	----	----	----	0.49	$7.94x10^{-11}$
353	0.43	$1.73x10^{-10}$	0.31	$6.02x10^{-09}$	0.37	$2.75x10^{-09}$	0.47	$8.71x10^{-11}$	0.34	$2.51x10^{-09}$	0.42	$2.18x10^{-9}$	0.41	$1.12x10^{-10}$
358	----	----	----	----	----	----	----	----	----	----	----	----	0.34	$8.31x10^{-10}$
363	----	----	0.32	$7.58x10^{-09}$	0.42	$3.38x10^{-09}$	0.39	$2.39x10^{-10}$	0.30	$7.94x10^{-09}$	0.46	$2.45x10^{-9}$	0.29	$2.34x10^{-9}$
368	----	----	----	----	----	----	----	----	----	----	----	----	0.26	$5.12x10^{-9}$
373	0.37	$1.02x10^{-9}$	0.39	$3.80x10^{-09}$	0.45	$3.16x10^{-09}$	0.41	$1.07x10^{-09}$	0.32	$1.31x10^{-08}$	0.54	$1.69x10^{-9}$	0.26	$7.24x10^{-9}$
378	----	----	----	----	----	----	----	----	----	----	----	----	0.29	$8.71x10^{-9}$
383	0.37	$3.23x10^{-9}$	0.52	$1.44x10^{-09}$	0.54	$1.47x10^{-09}$	0.49	$3.38x10^{-09}$	0.36	$1.41x10^{-08}$	0.52	$2.23x10^{-9}$	0.34	$6.61x10^{-9}$
393	0.37	$4.07x10^{-9}$	----	----	0.63	$8.12x10^{-10}$	0.52	$3.80x10^{-09}$	0.27	$2.29x10^{-08}$	0.44	$4.26x10^{-9}$	----	----
403	0.46	$1.44x10^{-9}$	----	----	----	----	----	----	0.29	$2.34x10^{-08}$	----	----	----	----
413	0.39	$2.63x10^{-9}$	----	----	----	----	----	----	----	----	----	----	----	----
423	0.38	$2.69x10^{-9}$	----	----	----	----	----	----	----	----	----	----	----	----

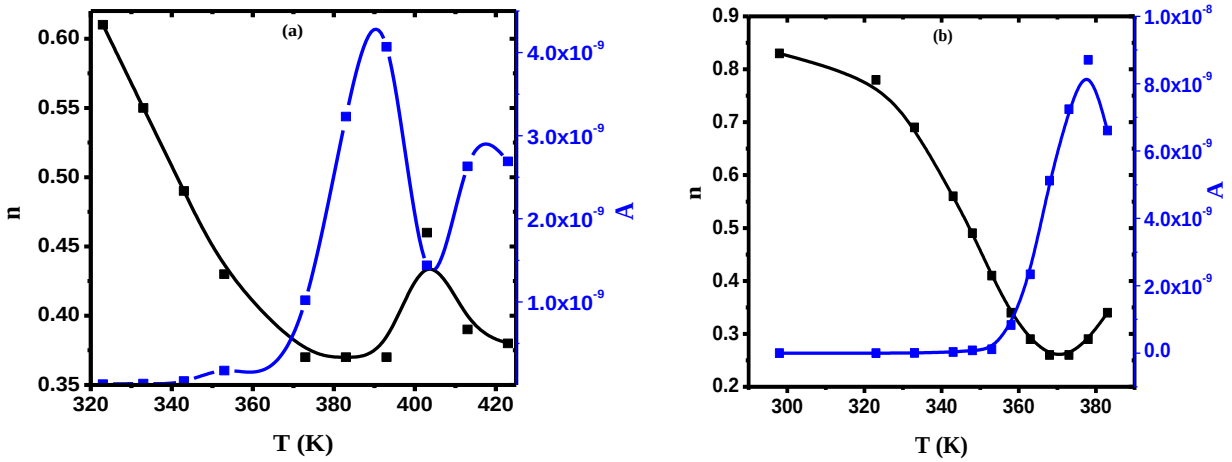

Fig. 6: The variation of the exponent n and the constant *A* with temperature for a) pure chitosan and b) pure PVA

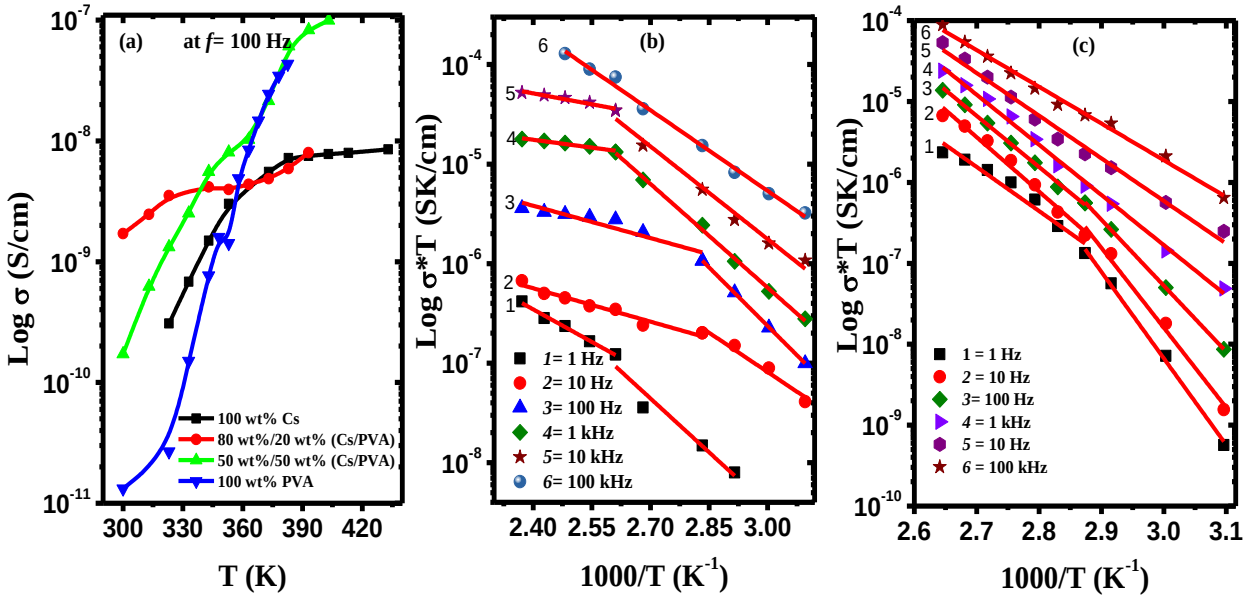

Fig. 7: a) The variation of electrical conductivity versus temperature for all samples at *f*= 100 Hz b) Log σT versus 1/T for pure chitosan (Cs) c) Log σT versus 1/T for pure PVA.

The activation energy (E_a) of conduction mechanism is estimated using Arrhenius's equation according to the following formula [31]

$$\sigma T = \sigma_0 \exp\left(-E_a / k_B T\right) \qquad (3)$$

Where σ_0, E_a and T are defined as a pre-exponential factor, conductivity activation energy and temperature, respectively. Fig. 7(b&c) depicts the variation of Log σT versus 1/T for chitosan and PVA at various frequencies. It is found that, the behavior of Log σT versus 1/T is characterized generally by two different regions with different slopes below and above glass transition (T_g) of each polymer. By knowing the slope of each region, the activation energy value of conduction has been calculated and summarized in Table 2 for all samples.

Cole-Cole plot is obtained when the real part (ε') of the complex permittivity (ε^*) is plotted on the x-axis and the imaginary part (ε'') on the y-axis. Fig. 8(a-e) displays Cole-Cole graphs (ε'' versus ε') of chitosan, PVA and 50/50 wt% (Cs/PVA) polyblend sample, respectively. Cole-Cole plot gives valuable information about the electrical performance of the materials in the form of semi circles. It is evident from Fig. 8 that the shapes of the Cole-Cole plots are of an imperfect semicircular nature. The depressed semicircular arc at high-frequency is associated to bulk conduction process. Hence, the presence of semicircle reveals that, there is no electrode interaction at the electrode interfaces, while only the conductivity relaxations effects can be observed. One can see that, pure chitosan showed two semicircles at higher temperatures, as shown in Fig. 8c, whereas, PVA exhibited nearly complete single semicircle with decreasing in its diameter with decreasing in temperature, as shown in Fig. 8d. The single semicircular arc expresses that there is one relaxation process involved in PVA. It is evident from Fig. 8 the relaxation process differs from the Debye relaxation process. Polymers are known to rarely follow the Debye relaxation theory and exhibit much wider dispersion due to the distribution of relaxation time. The incomplete semicircles at high temperatures describe the relaxation time distribution confirming the presence of non-Debye relaxation in the samples. The presence of two semicircles is a sign of the electrically inhomogeneous behavior of chitosan/PVA polyblend samples, as shown in Fig. 9 in the measured temperature range. The low-frequency semicircle is due to the effect of grain boundaries, or the so-called Maxwell-Wagner-Sillars relaxation. The changes observed in the shape of the Cole-Cole plots of polyblend samples, as shown in Fig. 9, may be due to the formation of perturbed polymeric chains due to the blending. The semicircles area of pure and polyblend samples and the shifting of the intercept of a semicircle towards higher value of ε' on the real axis of ε' with increasing the temperature represent an increase in the capacitance.

Table 2: Values of the activation energy, E_a (ev).

	Chitosan (Cs)		90/10 wt% (Cs/PVA)		80/20 wt% (Cs/PVA)		60/40 wt% (Cs/PVA)		50/50 wt% (Cs/PVA)		30/70 wt% (Cs/PVA)		PVA	
f (Hz)	E_{a1}	E_{a2}	E_{a1}	E_{a2}	E_{a1}	E_{a2}	E_{a1}	E_{a2}	E_{a1}	E_{a2}	E_{a1}	E_{a2}	E_{a1}	E_{a2}
1 Hz	0.31	0.19	0.17	0.31	0.33	----	0.18	0.49	0.26	0.52	0.29	0.56	0.92	0.47
10 Hz	0.23	0.10	0.06	0.25	0.003	0.25	0.21	0.44	0.27	0.56	0.34	0.55	0.85	0.58
100 Hz	0.38	0.10	0.16	0.06	0.11	0.08	0.24	0.24	0.31	0.36	0.61	0.36	0.70	0.72
1 kHz	0.30	0.04	0.24	0.08	0.13	0.07	0.21	0.25	0.29	0.27	.033	0.22	0.53	----
10 kHz	0.27	0.06	0.20	0.24	0.10	0.21	0.17	0.34	0.24	0.37	0.27	0.29	0.45	----
100 kHz	0.23	----	0.15	0.30	0.07	0.26	0.16	0.34	0.23	0.38	0.29	0.34	0.39	----

Cole-Cole behavior

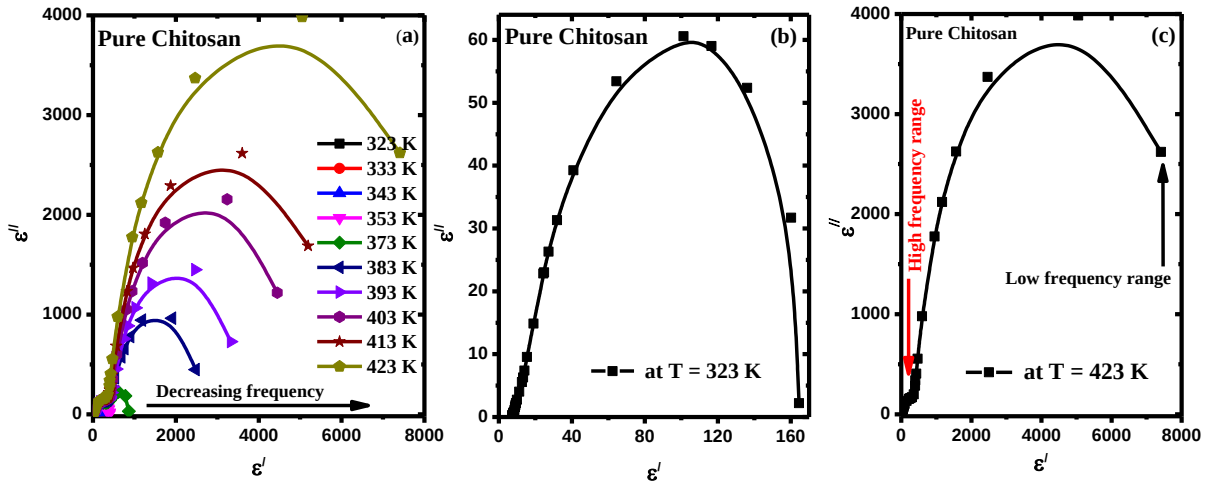

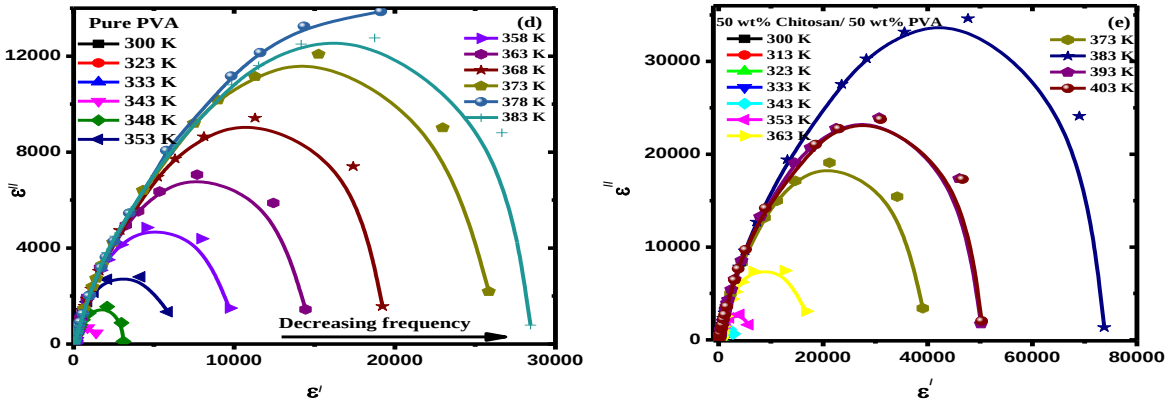

Fig. 8: Cole-Cole plot of: a-c) chitosan (Cs) d) PVA and e) 50wt% /50wt% (Cs/PVA).

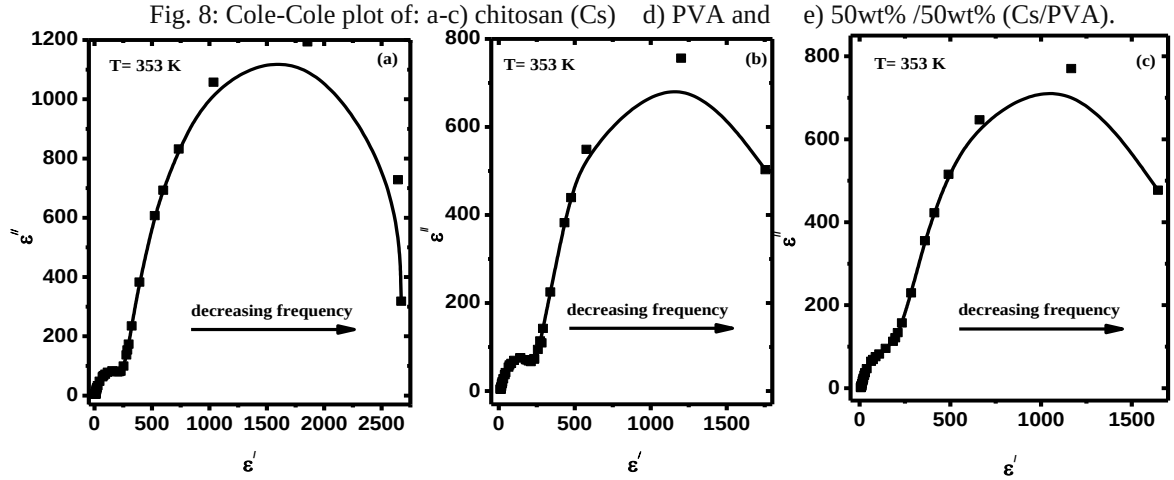

Fig. 9: Cole-Cole plot of a) 90/10 wt% (Cs/PVA) b) 80/20 wt% (Cs/PVA) and c) 60/40 wt% (Cs/PVA).

Electric Modulus

The electrical modulus is used to investigate the behavior of conduction and dielectric relaxation of polymer materials. Space charge polarization or MWS polarization leads to dielectric breakdown or partial discharge and the electrode polarization can lead to a large permittivity that makes it difficult to investigate the material behavior. Complex electric modulus (M^*) in these cases works as important a powerful tool for dealing with this type of problem.

The complex electric modulus (M^*) can be described in terms of the complex dielectric permittivity (ε^*) as follows:

$$M^*(\omega)=\frac{1}{\varepsilon^*(\omega)}=M^{/}+jM^{//}$$

$$=\frac{\varepsilon^{/}}{\varepsilon^{/2}+\varepsilon^{//2}}+j\frac{\varepsilon^{//}}{\varepsilon^{/2}+\varepsilon^{//2}} \qquad (4)$$

Where $M^{/}$ and $M^{//}$ are the real and imaginary parts of the complex electric modulus $M^*(\omega)$.

Spectra of electric modulus provide a great opportunity to examine the conductivity as well as the associated relaxation in polymers or ionic conductors [32,33]. Macedo *et al* used the electric modulus originally to investigate relaxation behavior of space charge [34]. It is associated with the relaxation of electric field in polymeric materials when the electric displacement remains constant. This means that, electric modulus explains the main reason of the dielectric relaxation process. A combined investigation of complex permittivity and modulus is useful for interpreting the conduction phenomena.

Fig. 10 displays the behavior of $M^{/}$ versus frequency at various temperatures of chitosan, PVA and its polyblend samples. It is observed that, the value of $M^{/}$ approaches to zero at lower frequencies indicating the negligible influence of electrode polarization [35].

At lower frequencies the presence of the long tail is attributed to the large capacitance associated with the electrodes, proving that the behavior is non-Debye [36]. On the other hand, the dispersion of $M^{/}$ at higher frequencies is observed, which may appear due to the relaxation conductivity. The continuous increase in values of $M^{/}$ obtained with increasing the frequency may has been resulted from the short range of charge carrier mobility.

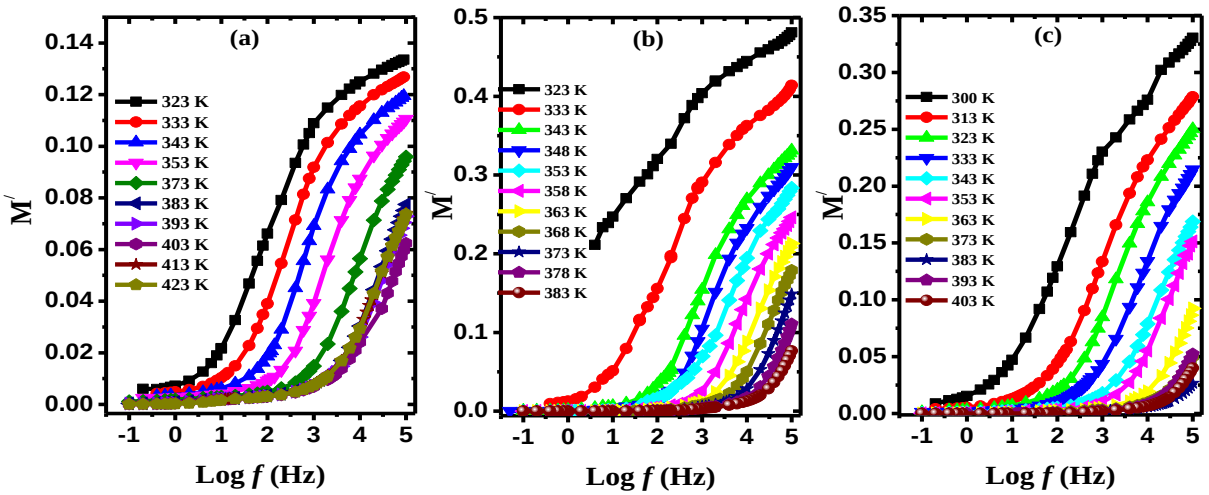

Fig. 10: M/ behavior versus frequency of a) chitosan (Cs), b) PVA and c) 50wt% /50wt% (Cs/PVA).

It is observed at high frequencies and low temperatures M/ for all samples tends to saturate. It is also noted that with increasing temperature the M/ values decreased, due to the fact that the mobility of charge carriers and movement of huge portion of the polymer molecular chains is increased with temperature. This behavior may be attributed to the nature of diminutive forces, which govern the movement of charge carrier under the influence of the induced electric field. Saturation of M/ values at higher frequencies indicates that the electrical properties of materials are frequency independent. The saturation of M/ at higher frequency may be due to non-existent dipole orientation [37]. Such behavior indicates that, these materials are very capacitive in nature [38]. No relaxation peak was observed in M/ spectra because M/ in complex electric modulus (M^*) is equivalent to $\varepsilon^/$ in complex permittivity (ε^*).

Fig. 11 shows M// behavior against frequency at various temperatures of chitosan, PVA and 50wt%/50wt% (Cs/PVA) polyblend sample. The behavior of M// exhibited well-resolved relaxation peaks at characteristic frequencies. The asymmetry nature of M// has been obtained in the dispersion region of M/ spectrum and the peak position is shifted with increasing the temperature towards high frequency side. The shift of these peaks indicated the transition from long-range mobility to short-range mobility has been occurred with increasing temperature as well as frequency. This is because the charge carriers at a low frequency below M''_{max} are in motion over a long distance as the electric field changes slowly until reaching M''_{max}. On the other hand, after reaching M''_{max} with increasing frequency, the electric field will change rapidly, causing the charge carriers to move over short distances [39]. The asymmetric in the broadness of relaxation peak suggests that, the relaxation process of the samples in the higher frequency range is not related to Debye relaxation [40]. Such behavior is coherent with Maxwell-Wagner-Sillars (MWS) system and is confirmed by the dielectric constant behavior, as mentioned before [41].

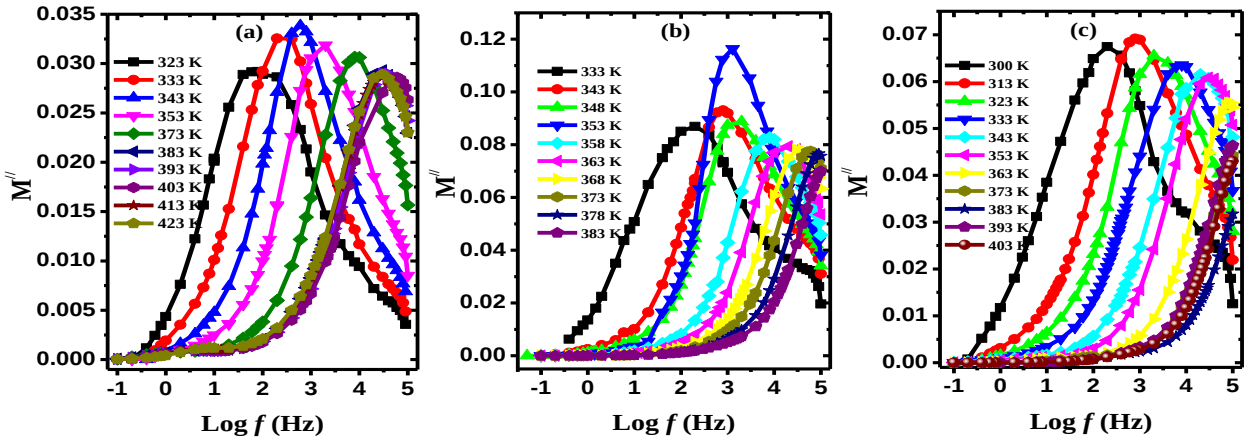

Fig. 11: M// behavior versus frequency of a) chitosan (Cs) b) PVA and c) 50wt%50wt% (Cs/PVA).

The shift of peak position towards high frequency side with increasing temperature in the spectra of M'' as shown in Fig. 11 revealed that, the process of dielectric relaxation is thermally activated [42]. Hence, we can conclude that with increasing temperature the relaxation time values will decrease. The shift of the relaxation peak gradually to higher frequency side can also be attributed to the segmental motion of the polymer backbone, i.e., dipolar relaxation (α-relaxation). The polyblend samples with a large difference in T_g values usually have broader dipolar relaxation peaks due to larger intrinsic mobility difference between different components of the two polymers.

Dipolar relaxation process of polysaccharides, such as chitosan, is explained generally as torsional oscillation between two rings of glucopyranose through a glucosidic oxygen and a cooperative reordering of hydrogen bonds because of functional groups activity (amides, amines and hydroxyls) as hydrogen bonds donors and acceptor [26]. On the other side, the dipolar relaxation peak of PVA is attributed to the cooperative local chain motion of PVA. Hydrogen bonds in PVA are the responsible and dominant interactions of molecular and structural dynamics. The existence of hydroxyl groups could strongly influence the properties of PVA because of the formation of inter-and intramolecular hydrogen bonds between OH and absorbed moisture or between OH groups [43].

The broadness of M'' in chitosan/PVA polyblend samples is a result of relaxation time distribution due to the heterogeneous behavior of the relaxed dipoles of polyblend samples. The relaxation time for all samples was estimated with the knowing of the frequency (f_{max}) corresponding to the maximum peak of the imaginary part of the electrical modulus (M''_{max}) which is referred to as relaxation frequency. The relaxation time values were calculated at different temperatures using the formula, $\tau = 1/2\pi f_{max}$

Fig. 12 depicts the Log τ variation against 1/T to calculate the activation energy values. From Fig. 12, we can observe clearly that the relaxation time of all samples exhibits a linear behavior against 1/T. The activation energy (E_a) values were calculated and listed in Table 3, according to the following equation

$$\tau = \tau_0 \exp\left(E_a / k_B T\right) \qquad (5)$$

Where τ_0 is pre-exponential factor and E_a, k_B and T are activation energy, Boltzmann's constant and absolute temperature, respectivelyIt is observed that with increasing PVA content the activation energy values increased, and this may be due to significant segmental mobility changes and a high degree of enhanced cooperation with the contribution of intra- and intermolecular hydrogen bond groups of chitosan and PVA. The interaction between chitosan and PVA is taken place through inter-chain hydrogen bonding between proton-acceptor groups, for instance C=O of chitosan and proton-donor groups, for instance OH/NH_2 and NH of chitosan and hydroxyl group (OH) of PVA polymer.

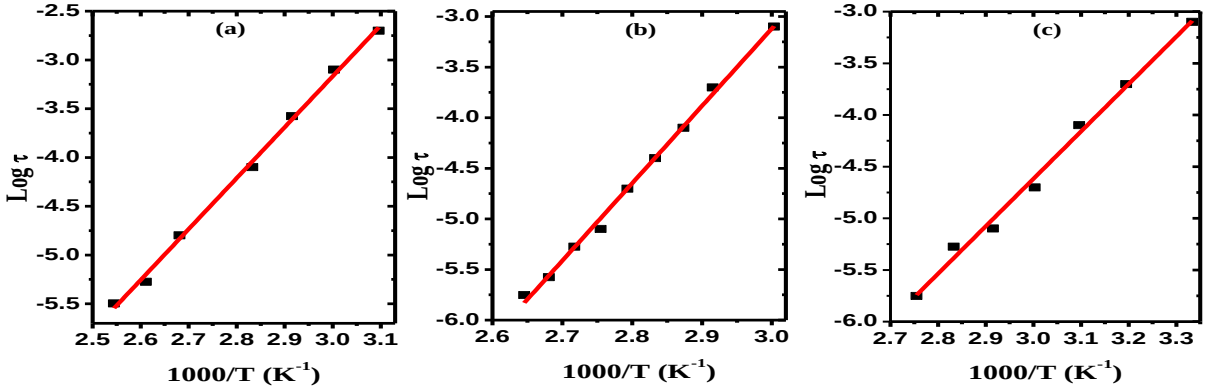

Fig. 12: Log τ versus 1/T of: a) chitosan (Cs) b) PVA and c) 50wt% /50wt% (Cs/PVA).

Table 3: Activation energy values and pre-exponential factor from M'' spectra.

Sample	E_a (eV)	τ_0 (sec)
Chitosan (Cs)	0.43	1.04×10^{-08}
90 wt% /10 wt% (Cs/PVA)	0.35	4.26×10^{-08}
80 wt% /20 wt% (Cs/PVA)	0.37	8.01×10^{-08}
60 wt% /40 wt% (Cs/PVA)	0.23	7.28×10^{-06}
50 wt% /50 wt% (Cs/PVA)	0.39	1.23×10^{-08}
30 wt% /70 wt% (Cs/PVA)	0.66	9.33×10^{-13}
PVA	0.67	2.91×10^{-12}

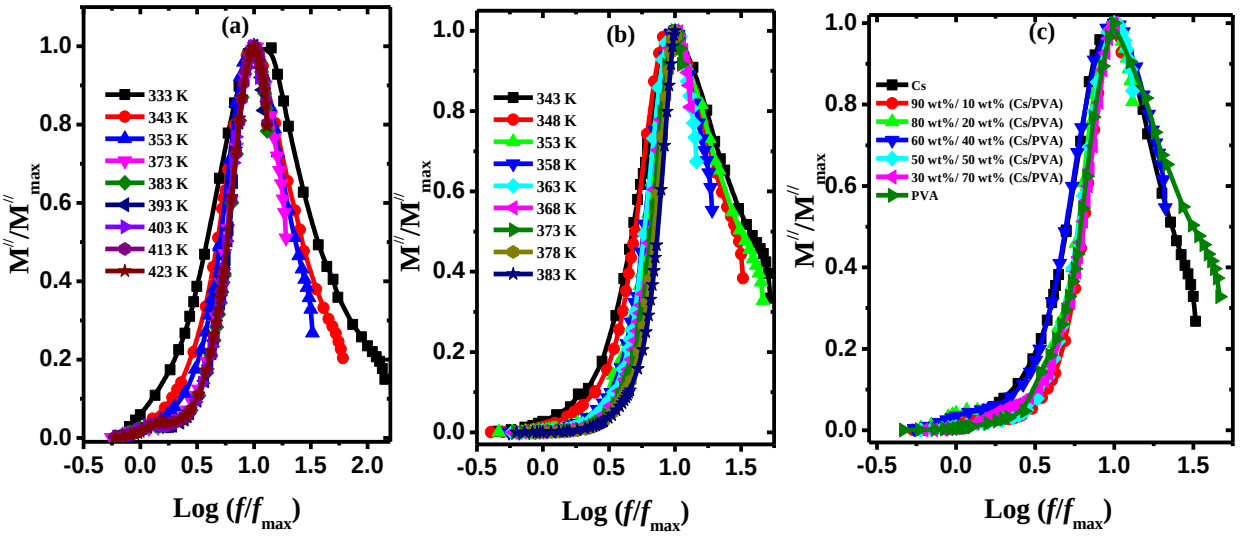

Fig. 13: Variation of M''/M''_{max} against log (f/f_{max}) of a) chitosan (Cs), b) PVA and c) polyblend samples at T= 333 K.

The spectrum of dielectric relaxation scaling is performed to display whether the relaxation process is dependent/independent of charge carrier concentration and/or thermally activated. The scaling behavior of the spectra of electric modulus gives us a deeper insight into the relaxation dynamics dependence on both composition and temperature. The scaling behavior of chitosan, PVA and polyblend samples has been carried out by plotting M''/M''_{max} at different temperatures versus Log(f/f_{max}) for pure samples, as shown in Fig 13(a&b). The scaling behavior of pure and polyblend samples has been plotted in Fig. 13c at T= 333 K, as a representative temperature. One can observe that, all the curves are overlapped indicating that, dynamic process is temperature independent [44]. The asymmetric obtained of the plots is a clear evidence of the asymmetric of relaxation times distribution and that the relaxation processes of chitosan/PVA dielectrics deviate from the behavior of Debye [45,13]. The dynamic process appearing at various frequencies reveals that the values of activation energy are not equal [46]. This behavior confirms that, the relaxation process has been taken place in the conductivity phenomenon of all samples.

Conclusion

The dielectric measurements of chitosan, PVA and its biopolymer blend revealed that, both ε' and ε'' have the same behavior. Higher values of ε' and ε'' are attributed at low frequencies and high temperatures to interfacial polarization and DC conduction. The dipolar relaxation process of both chitosan and PVA are observed around T_g in the isochronal behavior of ε''. The variation of the exponent *n* with temperature confirmed that, the conduction mechanism of chitosan/PVA is correlated with the overlapping-large polaron tunneling (OLPT) model. The observed incomplete semicircles of Cole-Cole plot described the distribution of relaxation time and confirming the presence of non-Debye relaxation in the samples. The asymmetric in the broadness of relaxation peak in M'' behavior suggested that, the relaxation process of the samples in the higher frequency range is not related to Debye relaxation. It is found that, the activation energy values are increased with increasing PVA content. This may be due to significant segmental mobility changes and a high degree of cooperativity enhanced by the contribution of intra and intermolecular hydrogen bonds assemblies of chitosan and PVA. The master curve of scaling behavior indicated that, dynamic relaxation process of chitosan, PVA and its polyblend samples is temperature independent.

Acknowledgement

M. T. Ahmed and T. Fahmy thanks Scientific Research Deanship (SRD) in Prince Sattam bin Abdulaziz University, KSA. Also, one of the authors (ZME) would like to thank Deanship of Scientific Research (DSR) in Princess Nourah bint Abdulrahman University, Saudi Arabia for funding this research through the fast-track research funding program.

References

1. Azuma K., Ifuku S., Osaki T., Okamoto Y., and Minami S., Preparation and biomedical applications of chitin and chitosan nanofibers, J. Biomed Nanotechnol., 10(10), 2891-920 (2014). doi: 10.1166/jbn.2014.1882.
2. Egginger M., and Schwoediauer R., Analysis of mobile ionic impurities in polyvinylalcohol thin films by thermal discharge current and dielectric impedance spectroscopy, AIP Adv., 2, 042152-15 (2012). https://doi.org/10.1063/1.4768805
3. Garrel D. R., Goudrea P., Zhang L., Reeves I., and Brazeau P., Chronic administration of growth

hormone-releasing factor increases wound strength and collagen maturation in granulation tissue, J. Surg. Res., 51, 297-302 (1991). https://doi.org/10.1016/0022-4804(91)90111-X
4. Stretz H. A., Paul D. R., and Cassidy P. E., Poly(styrene-*co*-acrylonitrile)/montmorillonite organoclay mixtures: a model system for ABS nanocomposites, Polymer, 46, 3818-3830 (2005). https://doi.org/10.1016/j.polymer.2005.03.043
5. Balart R., Lopez J., Garcia D., and Salvador M. D., Recycling of ABS and PC from electrical and electronic waste. Effect of miscibility and previous degradation on final performance of industrial blends. Eur. Polym. J., 41, 2150-2160 (2005). https://doi.org/10.1016/j.eurpolymj.2005.04.001
6. Zhang X., Chen S., Liu J., Hu Z., Chen S., and Wang L., Preparation and properties of sulfonated poly(phenylene arylene)/sulfonated polyimide (SPA/SPI) blend membranes for polymer electrolyte membrane fuel cell applications. J. Membr. Sci., 371, 276-285 (2011). https://doi.org/10.1016/j.memsci.2011.01.054
7. Hamed I., Özogul F., and Regenstein J.M., Industrial applications of crustacean by-products (chitin, chitosan and chitooligosaccharides): a review, Trends Food Sci. Technol., 48, 40–50 (2016). DOI: 10.1016/j.tifs.2015.11.007
8. Choo K., Ching Y. C., Chuah C. H., Julai S., and Liou N. S., Preparation and Characterization of Polyvinyl Alcohol-Chitosan Composite Films Reinforced with Cellulose Nanofiber. Materials, 9, 644-657 (2016). https://doi.org/10.3390/ma9080644
9. Migahed M. D., Ishra M., Fahmy T., and Barakat A., Electric modulus and AC conductivity studies in conducting PPy composite films at low temperature, J. Phys. Chem. Solids, 65, 1121-1125 (2004). DOI: 10.1016/j.jpcs.2003.11.039
10. Fahmy T., Dielectric Relaxation Spectroscopy of Poly (Vinyl Chloride-co-Vinyl Acetate-co-2-Hydroxypropyl Acrylate)/ Poly (Acrylonitrile-Butadiene-Styrene) Polymer Blend, Polym. Plast. Techn. & Eng., 46, 7-18 (2007). DOI: 10.1080/03602550600915136
11. Fahmy T., and Ahmed M. T., Dielectric Relaxation Spectroscopy of a Poly (Acrylonitrile-Butadiene-Styrene)/Styrene-Acrylonitrile Polymer Blend, J. of the Korean Phys. Soc., 58(6), 1654-1659 (2011). DOI: 10.3938/jkps.58.1654
12. Fahmy T., Ahmed M. T., El-kotp A., Abdelwahed H. G., and Alshaeer M. Y., Broadband Dielectric Spectroscopy and Electric Modulus Analysis of Poly (3-hydroxybutyrate-co-3-hydroxyvalerate) and Related Copolymers Films, Inter. J. of Phys. Appli., 8(1), 1-14 (2016).
13. Fahmy T., Ahmed M. T., Sarhan A., Abdelwahed H. G., and M. Alshaaer, AC Conductivity and Dielectric Spectroscopy of Poly (3-hydroxybutyrateco-3-hydroxyvalerate), Inter. J. of Applied Eng. Res., 11(18), 9279-9288 (2016).
14. Chen P., Xie F., Tang F., and McNally T., Structure and properties of thermomechanically processed chitosan/carboxymethyl cellulose/graphene oxide polyelectrolyte complexed bionanocomposites, Inter. J. of Bio. Macromolecules, 158(1), 420-429 (2020). https://doi.org/10.1016/j.ijbiomac.2020.04.259
15. Markiewicz E., Chybczyńska K., Zasadzińska A. G., Borysiak S., Wolak J., and Matczak M., Dielectric properties of the chitosan–spinel CoFe2O4 composites, Phase Transition, 1-14 (2018). https://doi.org/10.1080/01411594.2018.1519714
16. Krishnan S. K., Prokhorov E., and Barcenas G. L., Molecular relaxation in Chitosan films in GHz frequency range. Mater. Res. Soc. Symp. Proc., Materials Research Soc., 1613, 83-88 (2014). https://doi.org/10.1557/opl.2014.162
17. Fahmy T., Elhendawi H., Elsharkawy W. B., and Reicha F. M., AC conductivity and dielectric relaxation of chitosan/poly(vinyl alcohol) biopolymer polyblend. Bull. Mater. Sci., 43, 1–10 (2020). https://doi.org/10.1007/s12034-020-02207-2
18. Li Y.Q., Zhang C.X., Jia P., Zhang Y., Lin L., Yan Z.B., Zhou X.H., and Liu J.–M., Dielectric relaxation of interfacial polarizable molecules in chitosan ice-hydrogel materials, J. of Materiomics, 4(1), 35-43 (2018). https://doi.org/10.1016/j.jmat.2017.12.005
19. Johns J., Nakason C., Dielectric properties of natural rubber/chitosan blends: Effects of blend ratio and compatibilization, J. of Non-Cryst. Solids, 357(7), 1816-1821 (2011). https://doi.org/10.1016/j.jnoncrysol.2011.01.036
20. T. Fahmy and H. Elzanaty, AC conductivity and broadband dielectric spectroscopy of a poly(vinyl chloride)/poly(ethyl methacrylate) polymer blend", Bull. Mater. Sci., 42(5), 220-226 (2019). https://doi.org/10.1007/s12034-019-1906-1
21. Ishaq S., Kanwal F., Atiq S., Moussa M., Azhar U., Gul I., and Losic D., Dielectric and impedance spectroscopic studies of three phase graphene/titania/poly(vinyl alcohol) nanocomposite films, Results in Phys., 11, 540–548 (2018). https://doi.org/10.1016/j.rinp.2018.09.049
22. Fahmy T., and Sarhan A., Characterization and molecular dynamic studies of chitosan-iron complexes, Bull. Mater. Sci., 44, 142 (2021). https://doi.org/10.1007/s12034-021-02434-1S
23. Singh P., Gupta P.N., and Saroj A.L., Ion dynamics and dielectric relaxation behavior of PVA-PVP-NaI-SiO based nano-2 composites polymer blend electrolytes, Physica B: Phys. of Cond. Matt., 578(1), 411850 (2019). https://doi.org/10.1016/j.physb.2019.411850
24. Fahmy T., and Ahmed M. T., Alternating –Current Conductivity and Dielectric Relaxation of Poly (Acrylonitrile-Butadiene-Styrene) Terpolymer Doped with Tetrabutylammonium Tetrafluoroborate, J. Polym. Mater., 20, 367-376 (2003).
25. Mydhili V., and Manivannan S., Effect of microstructure on the dielectric properties of poly(vinyl alcohol)–poly(3,4-ethylenedioxythiophene) doped with poly(styrenesulfonate) composite films. J. Appl. Polym. Sci., 134, 45079 (2017). DOI: 10.1002/app.45079
26. Garrido I. Q., Gonzalez V. I., Arechederra J. M. M., and Rienda J. M. B., The role played by the interactions of small molecules with chitosan and their transition temperatures. Glass-forming liquids: 1,2,3-Propantriol (glycerol). Carbohydr. Polym., 68(1),

173–186 (2007). https://doi.org/10.1016/j.carbpol.2006.07.025
27. Fahmy T., Dielectric Relaxation and Electrical Conductivity Study in Thiourea-Doped Poly (Vinyl Alcohol), Inter., J. Polym. Mater., 50, 109-127 (2001). DOI: 10.1080/00914030108035094
28. Chen P., Xie F., Tang F., and McNally T., Structure and properties of thermomechanically processed chitosan/carboxymethyl cellulose/graphene oxide polyelectrolyte complexed bionanocomposites, Inter. J. of Biological Macromolecules, 158, 420-429 (2020). https://doi.org/10.1016/j.ijbiomac.2020.04.259
29. Ghosh A., Frequency-dependent conductivity in bismuth-vanadate glassy semiconductors, Phys. Rev. B41 1479 (1990). DOI:https://doi.org/10.1103/PhysRevB.41.1479
30. Long A. R., Frequency-dependent loss in amorphous semiconductors, Adv. Phys., 31, 553-637 (1982). https://doi.org/10.1080/00018738200101418
31. Masmoudi W., Kamoun S., and Gargouri M., AC conductivity and dielectric studies of (C5H10N)2BiCl5 compound, Ionics, 18, 117–126 (2012). DOI 10.1007/s11581-011-0601-z
32. Mukherjee P.S., Das A.K., Dutta B., and Meikap A.K., Role of silver nanotube on conductivity, dielectric permittivity and current voltage characteristics of polyvinyl alcohol-silver nanocomposite film, J. of Phys.&Chem. of Solids, 11, 266-273 (2017). https://doi.org/10.1016/j.jpcs.2017.07.032
33. Angell C. A., Dynamic processes in ionic glasses, Chem. Rev., 90, 523–542 (1990). https://doi.org/10.1021/cr00101a006
34. Macedo P. B., Moynihan C. T., and Bose R., The Role of Ionic Diffusion in Polarization in Vitreous Ionic Conductors. Phys. Chem. Glasses, 13, 171–179 (1972).
35. Afandiyeva I. M., Bülbül M. M., Altındal S., and Bengi S., "Frequency dependent dielectric properties and electrical conductivity of platinum silicide/Si contact structures with diffusion barrier", Microelectronic Eng., 93, 50-55 (2012). https://doi.org/10.1016/j.mee.2011.05.041
36. Sudhakar Y. N., Selvakumar M., and Bhat D. K., Preparation and characterization of phosphoric acid-doped hydroxyethyl cellulose electrolyte for use in supercapacitor, Mater Renew Sustain Energy, 4, 10 (2015). DOI 10.1007/s40243-015-0051-z
37. More S., Dhokne R., and Moharil S., Dielectric relaxation and electric modulus of polyvinyl alcohol–Zinc oxide composite films, Mater. Res. Express, 4, 055302-12 (2017). https://doi.org/10.1088/2053-1591/aa6b26
38. Costa M. M., Terezo A. J., Matos A. L., Moura W.A., Giacometti J. A., and Sombra A. S. B., Impedance spectroscopy study of dehydrated chitosan and chitosan containing $LiClO_4$, Physica B., 405, 4439–4444 (2010). https://doi.org/10.1016/j.physb.2010.08.011
39. Singh G., and Tiwari V., Effect of Zr concentration on conductivity behavior of (1–x) PMN-xPZ ceramic: an impedance spectroscopy analysis. J. Appl. Phys., 106(12), 124104 (2009). https://doi.org/10.1063/1.3270430
40. Sinha A., and Dutta A., Microstructure evolution, dielectric relaxation and scaling behavior of Dy-for-Fe substituted Ni nanoferrites, RSC Adv., 5, 100330–100338 (2015). https://doi.org/10.1039/C5RA14783B
41. Molak A., Paluch M., Pawlus S., Klimontko J., Ujma Z., and Gruszka I., Electric modulus approach to the analysis of electric relaxation in highly conducting $(Na0.75Bi0.25)(Mn0.25Nb0.75)O_3$ ceramics, J. Phys. D Appl. Phys., 38, 1450–1460 (2005). DOI: 10.1088/0022-3727/38/9/019
42. Marín-Genescà M., García-Amorós J., Mujal-Rosas R., Massagués L., and Colom X., Study and Characterization of the Dielectric Behavior of Low Linear Density Polyethylene Composites Mixed with Ground Tire Rubber Particles. Polymers, 12, 1075 (2020). DOI:10.3390/polym12051075.
43. Hernández M. C., Suárez N., Martínez L. A., Feijoo J. L., Mónaco S. L., and Salazar N., "Effects of nanoscale dispersion in the dielectric properties of poly(vinyl alcohol)-bentonite nanocomposites", Phys. Rev E., 77(5), 051801-10 (2008). https://doi.org/10.1103/PhysRevE.77.051801
44. Sahoo P.S., Panigrahi A., Patri S.K. and Choudhary R.N.P., Bull. Mater. Sci., 33(2), 129–134 (2010). https://doi.org/10.1007/s12034-010-0018-8
45. Psarras G. C., Manolakaki E., and Tsangaris G. M., "Dielectric dispersion and ac conductivity in-Iron particles loaded-polymer composites," Composites Part A: Appl. Sci. & Manufac., 34, 1187–1198 (2003). https://doi.org/10.1016/j.compositesa.2003.08.002
46. Singh D. N., Sinha T.P., and Mahato D. K., Electric modulus, scaling and ac conductivity of La_2CuMnO_6 double perovskite. J. Alloy. Comp., 729(30), 1226–1233 (2017). https://doi.org/10.1016/j.jallcom.2017.09.241